



Defense Threat Reduction Agency
8725 John J. Kingman Road, MS
6201 Fort Belvoir, VA 22060-6201



DTRA-TR-16-10

TECHNICAL REPORT

Phonon Confinement Effect in TiO_2 Nanoparticles as Thermosensor Materials

Distribution Statement A. Approved for public release; distribution is unlimited.

January 2018

HDTRA1-09-1-0046

Liping Huang

Prepared by:
Rensselaer Polytechnic
Institute
110 8th Street
Troy, NY 12180

DESTRUCTION NOTICE:

Destroy this report when it is no longer needed.
Do not return to sender.

PLEASE NOTIFY THE DEFENSE THREAT REDUCTION
AGENCY, ATTN: DTRIAC/ RD-NTF, 8725 JOHN J. KINGMAN ROAD,
MS-6201, FT BELVOIR, VA 22060-6201, IF YOUR ADDRESS
IS INCORRECT, IF YOU WISH IT DELETED FROM THE
DISTRIBUTION LIST, OR IF THE ADDRESSEE IS NO
LONGER EMPLOYED BY YOUR ORGANIZATION.

REPORT DOCUMENTATION PAGE				<i>Form Approved</i> OMB No. 0704-0188	
<small>Public reporting burden for this collection of information is estimated to average 1 hour per response, including the time for reviewing instructions, searching existing data sources, gathering and maintaining the data needed, and completing and reviewing this collection of information. Send comments regarding this burden estimate or any other aspect of this collection of information, including suggestions for reducing this burden to Department of Defense, Washington Headquarters Services, Directorate for Information Operations and Reports (0704-0188), 1215 Jefferson Davis Highway, Suite 1204, Arlington, VA 22202-4302. Respondents should be aware that notwithstanding any other provision of law, no person shall be subject to any penalty for failing to comply with a collection of information if it does not display a currently valid OMB control number. PLEASE DO NOT RETURN YOUR FORM TO THE ABOVE ADDRESS.</small>					
1. REPORT DATE (DD-MM-YYYY)		2. REPORT TYPE		3. DATES COVERED (From - To)	
4. TITLE AND SUBTITLE				5a. CONTRACT NUMBER	
				5b. GRANT NUMBER	
				5c. PROGRAM ELEMENT NUMBER	
6. AUTHOR(S)				5d. PROJECT NUMBER	
				5e. TASK NUMBER	
				5f. WORK UNIT NUMBER	
7. PERFORMING ORGANIZATION NAME(S) AND ADDRESS(ES)				8. PERFORMING ORGANIZATION REPORT NUMBER	
9. SPONSORING / MONITORING AGENCY NAME(S) AND ADDRESS(ES)				10. SPONSOR/MONITOR'S ACRONYM(S)	
				11. SPONSOR/MONITOR'S REPORT NUMBER(S)	
12. DISTRIBUTION / AVAILABILITY STATEMENT					
13. SUPPLEMENTARY NOTES					
14. ABSTRACT					
15. SUBJECT TERMS					
16. SECURITY CLASSIFICATION OF:			17. LIMITATION OF ABSTRACT	18. NUMBER OF PAGES	19a. NAME OF RESPONSIBLE PERSON
a. REPORT	b. ABSTRACT	c. THIS PAGE			19b. TELEPHONE NUMBER (include area code)

UNIT CONVERSION TABLE

U.S. customary units to and from international units of measurement^{*}

U.S. Customary Units	<div style="display: flex; align-items: center; justify-content: center;"> <div style="margin-right: 10px;"> </div> Multiply by </div> <div style="display: flex; align-items: center; justify-content: center;"> <div style="margin-right: 10px;"> </div> Divide by[†] </div>	International Units
Length/Area/Volume		
inch (in)	2.54 × 10 ⁻²	meter (m)
foot (ft)	3.048 × 10 ⁻¹	meter (m)
yard (yd)	9.144 × 10 ⁻¹	meter (m)
mile (mi, international)	1.609 344 × 10 ³	meter (m)
mile (nmi, nautical, U.S.)	1.852 × 10 ³	meter (m)
barn (b)	1 × 10 ⁻²⁸	square meter (m ²)
gallon (gal, U.S. liquid)	3.785 412 × 10 ⁻³	cubic meter (m ³)
cubic foot (ft ³)	2.831 685 × 10 ⁻²	cubic meter (m ³)
Mass/Density		
pound (lb)	4.535 924 × 10 ⁻¹	kilogram (kg)
unified atomic mass unit (amu)	1.660 539 × 10 ⁻²⁷	kilogram (kg)
pound-mass per cubic foot (lb ft ⁻³)	1.601 846 × 10 ¹	kilogram per cubic meter (kg m ⁻³)
pound-force (lbf avoirdupois)	4.448 222	newton (N)
Energy/Work/Power		
electron volt (eV)	1.602 177 × 10 ⁻¹⁹	joule (J)
erg	1 × 10 ⁻⁷	joule (J)
kiloton (kt) (TNT equivalent)	4.184 × 10 ¹²	joule (J)
British thermal unit (Btu) (thermochemical)	1.054 350 × 10 ³	joule (J)
foot-pound-force (ft lbf)	1.355 818	joule (J)
calorie (cal) (thermochemical)	4.184	joule (J)
Pressure		
atmosphere (atm)	1.013 250 × 10 ⁵	pascal (Pa)
pound force per square inch (psi)	6.984 757 × 10 ³	pascal (Pa)
Temperature		
degree Fahrenheit (°F)	[T(°F) - 32]/1.8	degree Celsius (°C)
degree Fahrenheit (°F)	[T(°F) + 459.67]/1.8	kelvin (K)
Radiation		
curie (Ci) [activity of radionuclides]	3.7 × 10 ¹⁰	per second (s ⁻¹) [becquerel (Bq)]
roentgen (R) [air exposure]	2.579 760 × 10 ⁻⁴	coulomb per kilogram (C kg ⁻¹)
rad [absorbed dose]	1 × 10 ⁻²	joule per kilogram (J kg ⁻¹) [gray (Gy)]
rem [equivalent and effective dose]	1 × 10 ⁻²	joule per kilogram (J kg ⁻¹) [sievert (Sv)]

^{*} Specific details regarding the implementation of SI units may be viewed at <http://www.bipm.org/en/si/>.

[†] Multiply the U.S. customary unit by the factor to get the international unit. Divide the international unit by the factor to get the U.S. customary unit.

Phonon Confinement Effect in TiO₂ Nanoparticles as Thermosensor Materials

Institution's name:	Rensselaer Polytechnic Institute
Institution's address:	110 8th Street, Troy, NY 12180
Principal Investigator:	Liping Huang
Position Title of PI:	Associate Professor
Mailing Address of PI:	MRC 202, 110 8th Street, Troy, NY 12180
Telephone Number of PI:	(518) 276-2174
Email of PI:	huangL5@rpi.edu
Grant number:	HDTRA1-09-1-0046
Period of Performance:	6/23/09-9/30/15
Final report:	September 2015

Abstract

TiO₂ or ZnO nanoparticles (NPs) have a very strong finite-size dependency in their Raman spectra or photoluminescence (PL) spectra due to the phonon confinement effect or the quantum confinement effect. Together with a fast grain growth kinetics and a high stability under high temperature and pressure, they can forensically retain the complete thermal history of an event. By spatially distributing these NPs during thermal events such as blasts or weapon tests, a spatially and temporally non-uniform thermal environment can be determined by a direct read off their Raman or PL spectra at various locations. These thermosensors can also be used in non-defense applications such as for detecting the transient heating in electronics and measuring the rapid energy release during catastrophic fractures. The protocols developed in this project can be easily extended to the design of other thermosensors where a grain growth or phase transition at lower temperatures is needed to characterize the thermal environment on the biological or cellular level.

Objective

The objective of this research is to utilize the phonon/quantum confinement effect in Raman/PL spectra and grain growth kinetics in NPs as thermosensor materials, which allow us to forensically retain the complete thermal history (spatial and temporal variation) of a thermal event under extreme conditions.

Approach

We have been searching for NPs and substrates that meet the following requirements as thermosensor materials:

NPs:

- 1) Strong phonon/quantum confinement effect
- 2) Fast growth kinetics
- 3) Easy synthesis to get spherical NPs
- 4) High thermal and mechanical stability

Substrates as NPs' carrier and protector:

- 1) High thermal and mechanical stability
- 2) High thermal conductivity

We synthesized small and monodisperse TiO₂ and ZnO NPs of 5-6 nm in size and loaded them onto SBA-15 or graphite nanoplatelets (GNPs) substrates. Raman and PL spectrometers were used to establish the particle size versus the Raman/PL peak position master curves. Systematic isothermal and temperature-dependent heat treatments of NPs using a ribbon pyroprobe microheater (Fig. 1) were carried out to study their grain growth kinetics.

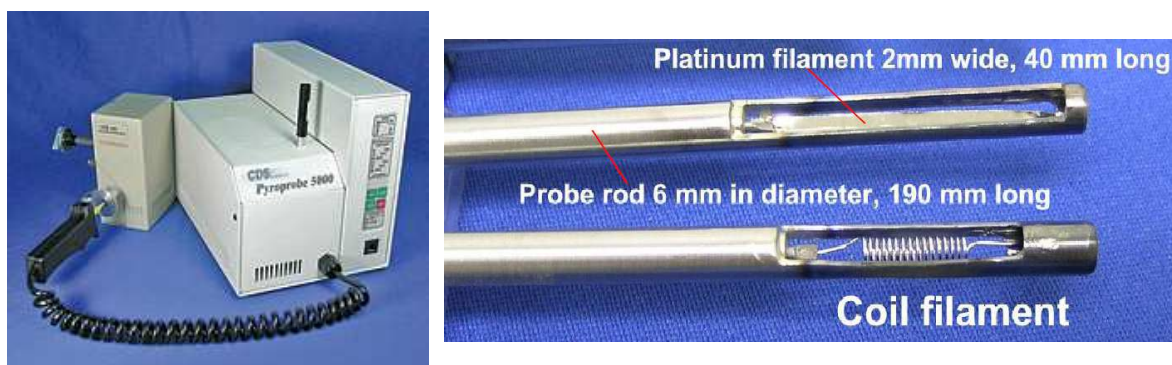


Fig. 1. Ribbon pyroprobe microheater from the CDS analytical, Inc., which can be heated from room temperature to 1400 °C with heating rates from 0.01 °C/min to 20,000 °C/s.

Work accomplished

We first explored bare TiO_2 and ZnO NPs as thermal sensors as they can be easily synthesized into spherical NPs (Fig. 2), and have strong phonon confinement in Raman spectrum (Fig. 3, left) and quantum confinement in PL spectrum (Fig. 3, right), respectively.

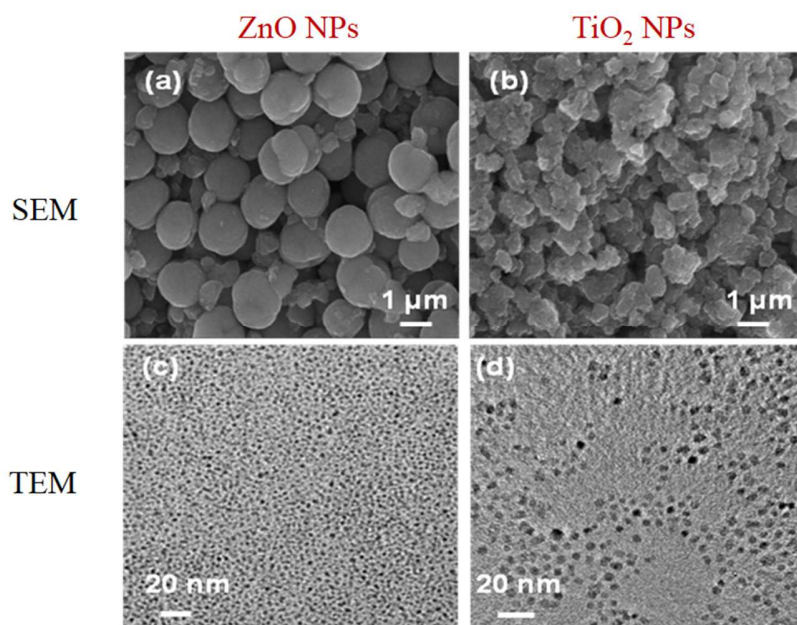


Fig. 2. SEM and TEM image of ZnO and TiO_2 NPs.

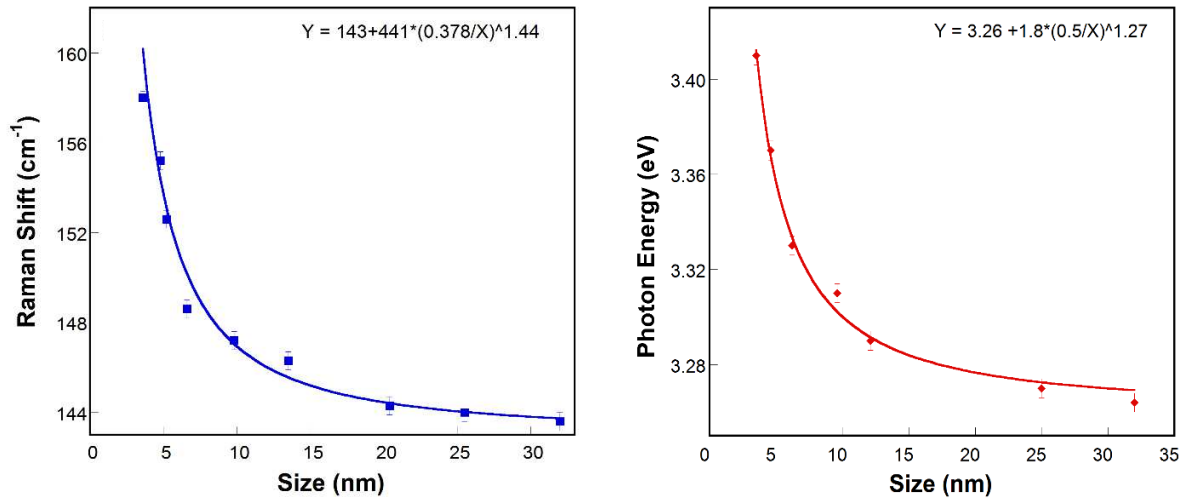


Fig. 3. Raman E_g band peak position of TiO_2 (left) and band gap of ZnO NPs (right) versus the NPs size.

Raman/PL spectra for TiO_2/ZnO after the constant temperature and constant time heat treat were taken and used to estimate the particle size from the master curves and used to fit the grain growth parameters for TiO_2 and ZnO , respectively:

$$\text{TiO}_2 \quad D^2 = D_0^2 + 1.4 \times 10^6 t^{1.11} e^{\left(-\frac{89}{RT}\right)} \quad (1)$$

$$\text{ZnO} \quad D^2 = D_0^2 + 7.4 \times 10^4 t^{0.88} e^{\left(-\frac{71}{RT}\right)} \quad (2)$$

We heat treated TiO_2 and ZnO NPs under various conditions, afterwards the particle sizes were estimated from the master curves and substituted into equation (1) and (2) to extract T and t , respectively. Calculated temperature and time are listed in Table 1.

Table 1. Temperature and time measurements from grain growth kinetics.

number	Setting T/t (K/s)	Calculated T/t (K/s)
1	823/15	812/16
2	853/10	867/9
3	773/60	795/53
4	873/30	855/34
5	973/5	948/6

We demonstrate that both temperature and time can be determined simultaneously by using NPs as thermosensors in the range of 400-700°C and 5-60 s, assuming that the temperature is constant (a step-function approximation to a thermal spike) during a thermal event.

Then we loaded TiO_2 and ZnO NPs of different sizes onto SBA-15 and GNP. Both substrates act like a carrier and protector for NPs, but do not interfere with the Raman/PL spectra of NPs as demonstrated in Fig. 4.

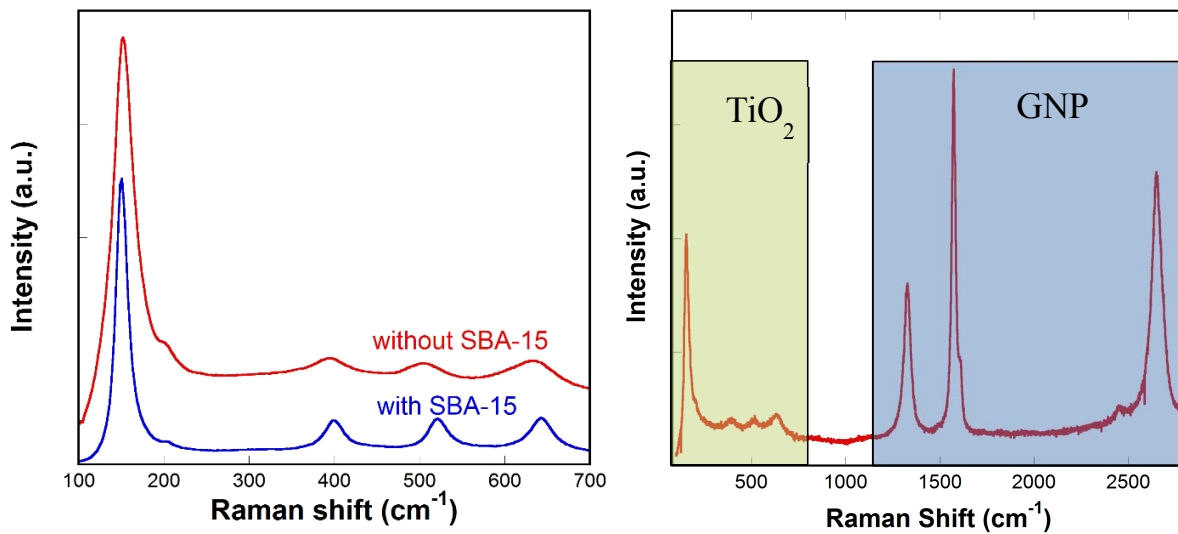


Fig. 4. Raman spectrum of anatase TiO_2 NPs with and without SBA-15 substrate (left), Raman spectrum of TiO_2 -GNP nano-composite (right).

A clear shift in Raman spectrum is seen in anatase TiO_2 NPs loaded onto SBA-15 after a heat treatment at 700°C for 0.3 s (Fig. 5).

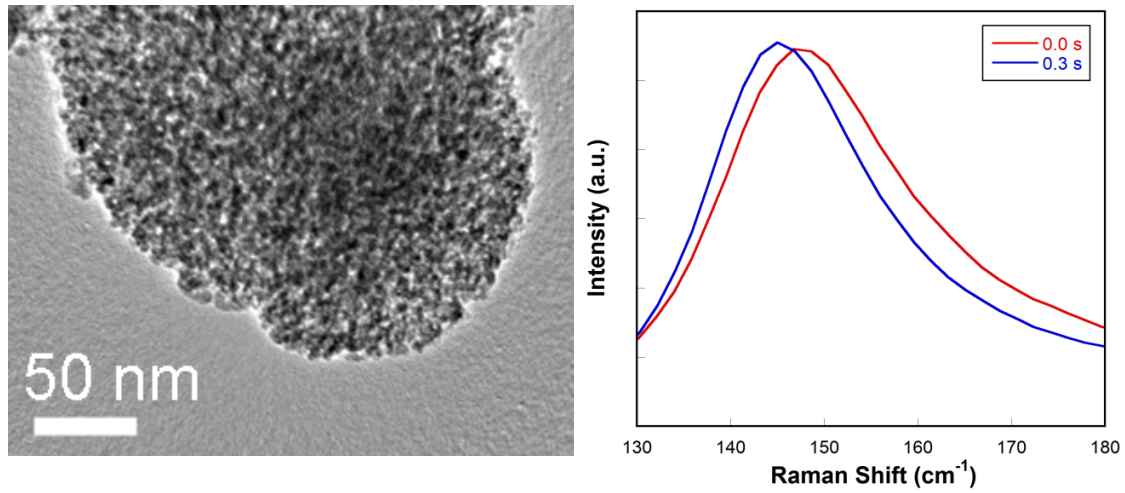


Fig. 5. (Left) TEM image of SBA-15 loaded with anatase TiO₂ NPs; (right) Raman spectrum of anatase TiO₂ NPs loaded in SBA-15 before and after a heat treatment at 700 °C for 0.3 s.

SBA-15 is good for its thermal stability, but its thermal conductivity is low (<1 W/mK), which limits NPs growth during a thermal event. We then tried to use GNP as the carrier, which has high thermal stability and high thermal conductivity (~ 300 W/mK). We decorated TiO₂ NPs over GNPs (Fig. 6) and studied the effect of substrate on their phonon confinement, grain growth and phase stability at high temperatures (Fig. 7 and 8). Thermal sensitive Raman signature, indicating the ultrafast grain growth of TiO₂ NPs in response to short thermal shock treatments (0.1-25 s) at high temperatures, was exploited for high temperature thermal sensing applications based on the phonon confinement effect.

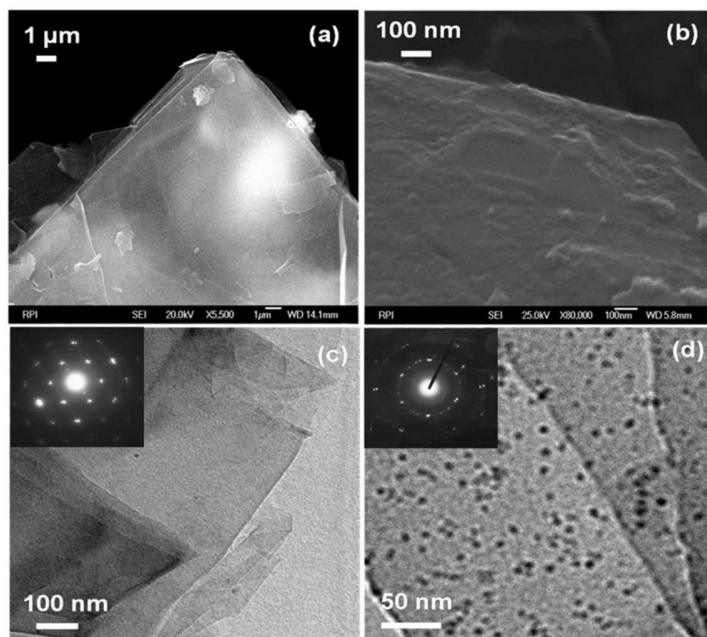
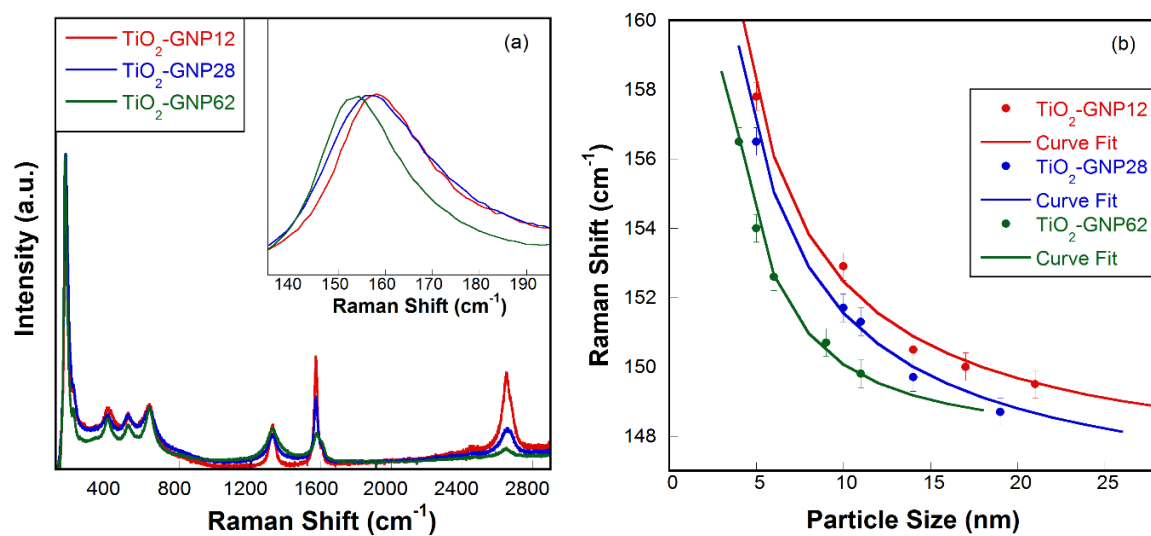


Fig. 6. SEM image of (a) GNP12 and (b) TiO_2 -GNP12 nanocomposite, TEM image of (c) GNP12 and (d) TiO_2 -GNP12 nanocomposite. Inset images indicate the corresponding SAED patterns.



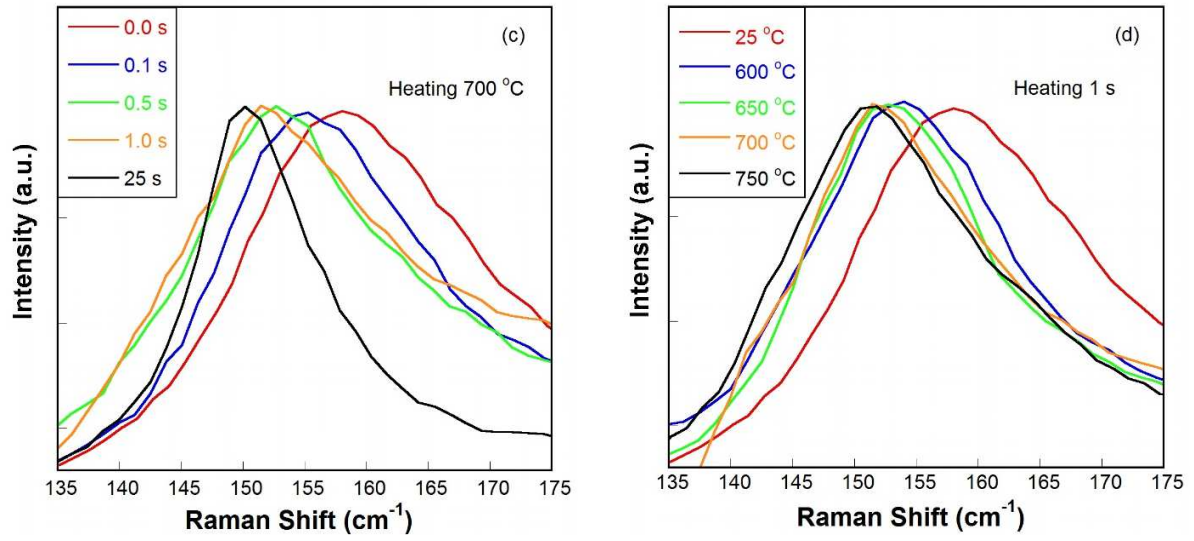


Fig. 7. (a) Raman spectra of TiO_2 -GNPs nanocomposites and (b) phonon confinement in TiO_2 -GNPs nanocomposites. Note: inset in (a) shows the Eg band of anatase TiO_2 , its position versus the particle size is shown as the master curve in (b) for each nanocomposite. Raman spectra of TiO_2 -GNP12 nanocomposite after heat treated (c) at 700°C for different times and (d) for 1 s at different temperatures.

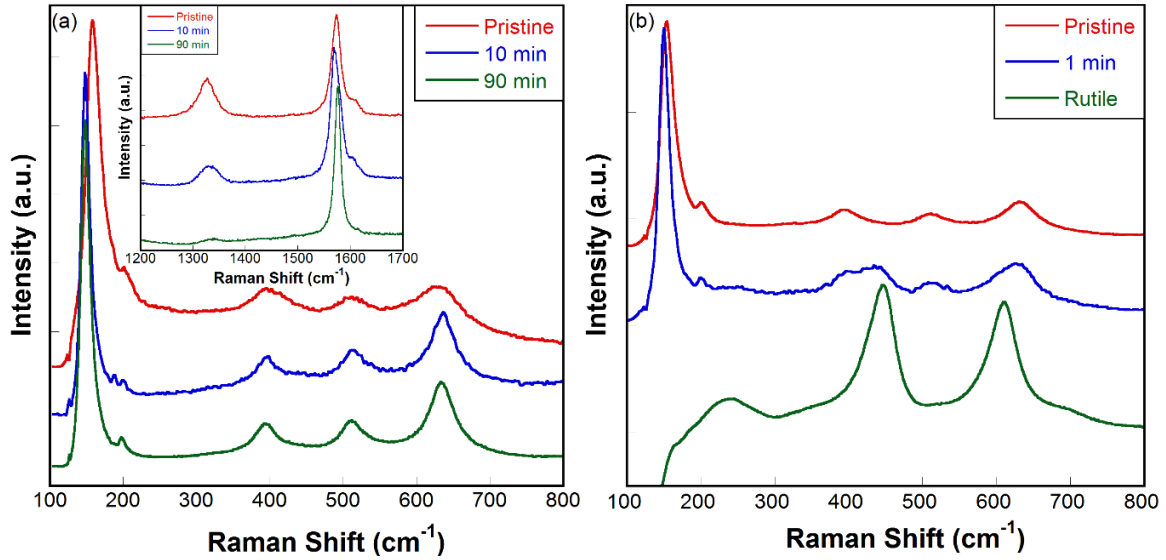


Fig. 8. Raman spectra of TiO_2 in (a) TiO_2 -GNP12 (inset shows the D- and G-band of GNPs) and (b) TiO_2 -GNP62 nanocomposites heated at 700°C for different durations. Raman spectrum of rutile phase is shown in (b) for comparison.

Some of our thermal sensors were sent to test in a shock tube in Dr. Nick Glumac's group at UIUC, which survived in the wash down process and showed the expected grain grown after being tested at 690 K (Fig. 9).

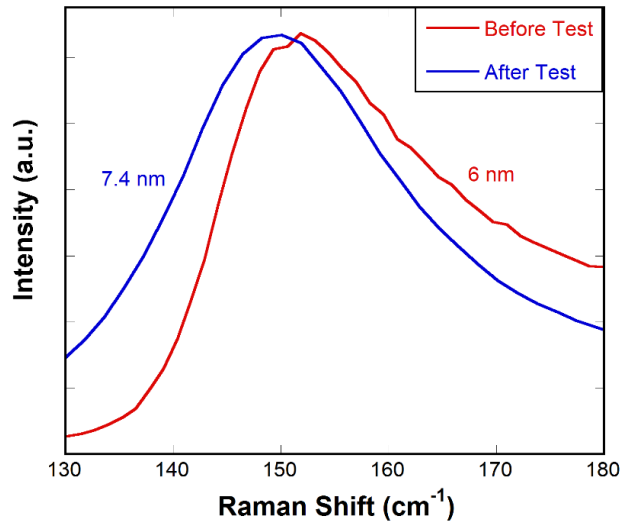


Fig. 9. Raman spectra of TiO₂ NPs before and after being tested in a shock tube at 690 K.

We also mixed some of our thermal sensors with detonation debris, which does not affect the Raman spectrum of NPs (Fig. 10).

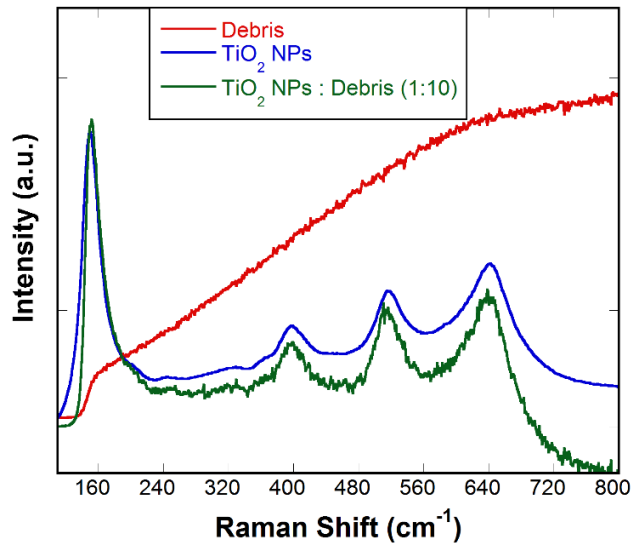


Fig. 10. Raman spectra of TiO₂ NPs with and without detonation debris.

Key outcomes

Our study showed that bare TiO₂ and ZnO NPs can be used as thermal sensors to extract both temperature and time. They are likely to perform better in static applications where NPs can stay together for grain growth to take place during thermal events. For dynamic applications, it is better to decorate NPs onto substrates, which act like a carrier and protector to keep NPs together during thermal events.

We demonstrated higher thermal stability of anatase TiO₂ NPs in TiO₂-GNPs nanocomposites compared to bare TiO₂ NPs for high temperature thermal sensor applications. Thermal shock responsive grain growth and Raman signature of TiO₂ in these nanocomposites enable them to map the temperature of harsh environments with a high accuracy of nearly 99% for a given short-time thermal exposure.

Our study showed that thermal sensors based on TiO₂ and ZnO NPs perform well under harsh test conditions, can be retrieved using wash down process and show strong signal among detonation debris. They have great potential as thermal sensors in field applications, where a spatially and temporally non-uniform thermal environment can be determined by a direct read off their Raman or PL spectra at various locations.

Papers published

- 1) Junwei Wang and Liping Huang, "Thermometry based on phonon confinement effect in nanoparticles", *Applied Physics Letters*, 98, 113102 (3 pages) (2011). Reprinted in the *Virtual Journal of Nanoscale Science & Technology* (March 28, 2011).
- 2) Junwei Wang, Ashish Kumar Mishra, Qing Zhao and Liping Huang, "Size Effect on Thermal Stability of Nanocrystalline Anatase Titanium Oxide", *Journal of Physics D: Applied Physics*, 46, 255303 (10 pages) (2013).
- 3) Ashish Kumar Mishra, Junwei Wang and Liping Huang, "Thermal sensitive quantum and phonon confinements for temperature mapping in extreme environments", *Journal of Physical Chemistry C*, 118 (13), 7222–7228 (2014).
- 4) Hongtao Sun, Xiang Sun, Mingpeng Yu, Ashish Kumar Mishra, Liping Huang, and Jie Lian, "Silica-Gold Core-Shell Nanosphere for Ultrafast Dynamic Nanothermometer", *Advanced Functional Materials*, 24(16), 2389–2395 (2014).
- 5) Ashish Kumar Mishra and Liping Huang, "TiO₂ Decorated Graphite Nanoplatelets Nanocomposites for High Temperature Sensor Applications", *Small*, 11, 361-366 (2015).
- 6) Ashish Kumar Mishra and Liping Huang, "Substrate effect on phonon confinement in TiO₂ nanoparticles for thermal sensing application", *Applied Physics Letters*, 105, 113104 (2014).
- 7) Ashish Kumar Mishra, K.V. Lakshmi and Liping Huang, "Eco-friendly Scalable Production of Metal Dichalcogenides Nanosheets and Their Visible Light Responsive Photocatalytic Applications", *Scientific Reports*, under review (2015).

Presentations given at national and international conferences

- 1) Ashish Kumar Mishra and Liping Huang, "Intrinsic Phonon/quantum confinement effect in nanoparticles as thermosensors", **MRS Fall Meeting**, Boston, MA, 2012.
- 2) Liping Huang, "Phonon/Quantum Confinement Effect in Nanoparticles as Thermosensor Materials", **Workshop on Time-Dependent Temperature Measurements in Energy Release Processes**, Chicago, IL, 2012.

- 3) Ashish Kumar Mishra and Liping Huang, "TiO₂ decorated graphite nanoplatelets- A high temperature thermal sensor material", **MS&T'14**, Pittsburgh, PA, 2014.
- 4) Ashish Kumar Mishra and Liping Huang, "TiO₂ decorated graphene like nanoflakes- A high temperature thermal sensor material", **New Diamond and Nano Carbon Conference**, Chicago, IL, 2014.
- 5) Ashish Kumar Mishra and Liping Huang, "Quantum confinement at nanoscale and its use in thermal mapping", **CRES Annual Meeting**, Troy, NY, 2014.

Personnel training and professional development

Three postdoctoral researchers: Dr. Junwei Wang (March 2010-September 2011), Dr. Ashish Mishra (January 2012-December 2014 and Dr. Michael Guerette (January-May 2015) were trained in developing thermal sensors.

One graduate student (Qing Zhao) finished his Ph.D degree and two graduate students (Garth Scannell and Siva Priya Jaccani) are working toward their Ph.D. degree, who have been partially supported by this project.

While working on this project, the PI, Liping Huang was promoted to associate professor with tenure at RPI, and received the following award/honor:

- The Alfred H. Geisler Memorial Award from the Eastern NY ASM Chapter, 2013
- National Science Foundation (NSF) CAREER award, 2013
- Inaugural Gordon S. Fulcher Distinguished Scholar from the Corning Incorporated, 2015

DISTRIBUTION LIST
DTRA-TR-16-10

DEPARTMENT OF DEFENSE

DEFENSE THREAT REDUCTION
AGENCY
8725 JOHN J. KINGMAN ROAD
STOP 6201
FORT BELVOIR, VA 22060
ATTN: D. DALTON

DEFENSE TECHNICAL
INFORMATION CENTER
8725 JOHN J. KINGMAN ROAD,
SUITE 0944
FT. BELVOIR, VA 22060-6201
ATTN: DTIC/OCA

DEPARTMENT OF DEFENSE
CONTRACTORS

QUANTERION SOLUTIONS, INC.
1680 TEXAS STREET, SE
KIRTLAND AFB, NM 87117-5669
ATTN: DTRIAC